

InterCLIP-MEP: Interactive CLIP and Memory-Enhanced Predictor for Multi-modal Sarcasm Detection

Junjie Chen¹, Subin Huang^{1*}

¹ Key Laboratory of Computer Application Technology
School of Computer and Information, Anhui Polytechnic University, Anhui, China

Abstract

The prevalence of sarcasm in social media, conveyed through text-image combinations, presents significant challenges for sentiment analysis and intention mining. Current multi-modal sarcasm detection methods have been proven to struggle with biases from spurious cues, leading to a superficial understanding of the complex interactions between text and image. To address these issues, we propose InterCLIP-MEP, a robust framework for multi-modal sarcasm detection. InterCLIP-MEP introduces a refined variant of CLIP, Interactive CLIP (InterCLIP), as the backbone, enhancing sample representations by embedding cross-modality information in each encoder. Furthermore, a novel training strategy is designed to adapt InterCLIP for a Memory-Enhanced Predictor (MEP). MEP uses dynamic dual-channel memory to store valuable historical knowledge of test samples and then leverages this memory as a non-parametric classifier to derive the final prediction. By using InterCLIP to encode text-image interactions more effectively and incorporating MEP, InterCLIP-MEP offers a more robust recognition of multi-modal sarcasm. Experiments demonstrate that InterCLIP-MEP achieves state-of-the-art performance on the MMSD2.0 benchmark. Code and data are available at <https://github.com/CoderChen01/InterCLIP-MEP>.

Introduction

Sarcasm, with its inherent subtlety and complexity, plays a significant role in human communication by often conveying irony, mockery, or hidden intentions (Muecke 1982; Gibbs and O’Brien 1991; Gibbs and Colston 2007). The automatic detection of sarcasm from text has been a significant research focus, aiding tasks such as sentiment analysis and intent mining (Pang, Lee et al. 2008; Tsur, Davidov, and Rappoport 2010; Bouazizi and Ohtsuki 2015; Poria et al. 2016; Amir et al. 2016; Wu et al. 2018; Tay et al. 2018; Baziotis et al. 2018). With the rapid development of social media platforms like Twitter and Reddit, the need for multi-modal sarcasm detection has become increasingly apparent. Users frequently use text-image combinations to convey their messages, making it essential to develop methods to interpret these multi-modal communications. The task of multi-modal sarcasm detection presents significant challenges, requiring the system to accurately capture and com-

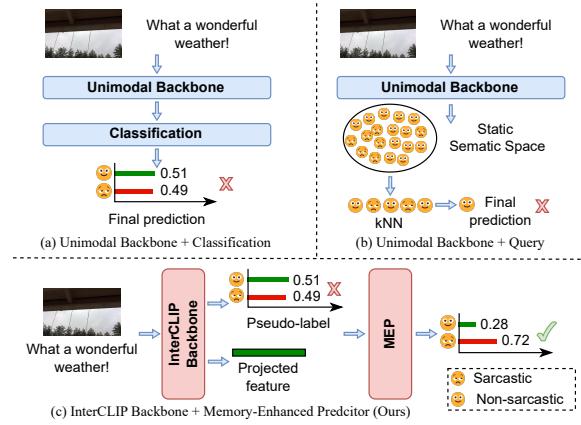


Figure 1: Comparison of InterCLIP-MEP and other multi-modal sarcasm detection pipelines.

prehend the intricate interplay between textual and visual information to identify sarcasm cues.

A pivotal development in this field was the introduction of the Multi-Modal Sarcasm Detection (MMSD) benchmark by Cai, Cai, and Wan (2019). This benchmark has become a cornerstone for subsequent research, inspiring a range of advanced techniques aimed at improving sarcasm detection performance (Xu, Zeng, and Mao 2020; Pan et al. 2020; Liang et al. 2021, 2022; Liu, Wang, and Li 2022; Wen, Jia, and Yang 2023; Tian et al. 2023; Wei et al. 2024). The above methods have explored various approaches, including the use of Transformer-based models for high-quality representation extraction (Pan et al. 2020), OCR and object detection technologies to enhance image understanding (Qiao et al. 2023), and the incorporation of external emotional knowledge (Liu, Wang, and Li 2022). Graph neural networks have also been utilized to construct dependency and cross-modal graphs for improved sarcasm identification (Liu, Wang, and Li 2022; Liang et al. 2021, 2022).

Despite these advancements, the existing methods have shown limitations, often learning biases from spurious cues present in the MMSD benchmark (Qin et al. 2023). To address this, Qin et al. (2023) introduced MMSD2.0, a refined benchmark that eliminates these spurious cues and corrects mislabeled samples. Their work demonstrated the need for

*Corresponding author. Email: {subinhuang@ahpu.edu.cn}

more reliable benchmarks and robust detection methods.

Building on these insights, we propose InterCLIP-MEP, a novel framework designed to enhance the reliability of multi-modal sarcasm detection. We present a comparison of existing methods with InterCLIP-MEP in Figure 1. As shown in Figure 1(a) and Figure 1(b), some existing methods use separate uni-modal encoders, such as BERT (Devlin et al. 2019) for text and ViT (Dosovitskiy et al. 2020) for visual modalities, as backbones (Xu, Zeng, and Mao 2020; Pan et al. 2020; Liang et al. 2021, 2022; Wen, Jia, and Yang 2023; Tian et al. 2023; Wei et al. 2024). These encoded samples are fused using various techniques to obtain the final sample representations. We argue that this approach makes it difficult for the model to capture the subtle interactive information between text and images. Although Qin et al. (2023) utilized a multi-modal pre-trained backbone, CLIP (Radford et al. 2021), to encode samples and demonstrated notable results on the MMSD2.0 benchmark, the original CLIP only aligns text and images directly, lacking the nuanced semantic space required for sarcasm detection. Therefore, InterCLIP-MEP introduces a refined variant, Interactive CLIP (InterCLIP), as the backbone to enhance sample encoding for this specific task. Inspired by the foundational work of Ganz et al. (2024), InterCLIP enhances the capture of interactive information between text and image by embedding representations from one modality into the encoder of the other, leading to a more nuanced understanding of multi-modal sarcasm cues.

After encoding the samples, as depicted in Figure 1(a), many approaches directly identify sarcastic samples through a classification module. This often leads to high prediction entropy and incorrect results, especially for hard cases with greater uncertainty. To the best of our knowledge, few methods consider leveraging historical knowledge of samples to aid in detection. As shown in Figure 1(b), only Wei et al. (2024) constructed a static semantic space that stores representations of all training samples. When identifying sarcastic samples, they query k -nearest neighbors in this semantic space and use a voting mechanism to derive the final predictions. However, their static semantic space struggles to handle out-of-distribution issues.

As shown in Figure 1(c), InterCLIP-MEP uses a novel training strategy to adapt InterCLIP for a Memory-Enhanced Predictor (MEP). Based on the sample representations encoded by InterCLIP, InterCLIP-MEP trains a classification module to assign pseudo-labels to samples. Simultaneously, it trains a projection module to map samples into a latent space. In this latent space, same-class samples are pulled closer together, while different-class samples are pushed further apart. Additionally, InterCLIP-MEP fine-tunes the weights of the self-attention modules in InterCLIP’s text and vision encoders using LoRA (Hu et al. 2022), building upon the original CLIP weights. Building on InterCLIP and its training strategy, MEP leverages historical knowledge of test samples to identify sarcasm. It maintains a dynamic, fixed-length dual-channel memory, with one channel storing historical information of non-sarcastic samples and the other storing information of sarcastic samples. MEP uses the learned InterCLIP to extract sample representations, calcu-

late pseudo-labels with the classification module, and compute prediction entropy, while also obtaining projection features through the projection module. Based on the pseudo-labels and prediction entropy, MEP dynamically updates the projected features of samples into the corresponding memory channels, treating these features as the historical knowledge of the test samples. Specifically, MEP consistently updates the memory with projected features of samples that have lower prediction entropy. MEP utilizes this memory as a non-parametric classifier to compute the final prediction for each sample.

Our experiments demonstrate the robustness and innovation of InterCLIP-MEP in accurately identifying sarcasm through sophisticated interaction and memory mechanisms. Our contributions can be summarized as follows:

- We propose InterCLIP-MEP, a novel framework for reliable multi-modal sarcasm detection, which introduces a refined variant of CLIP, Interactive CLIP (InterCLIP), as the backbone, improving the encoding of text-image interactions by embedding cross-modality information within each encoder.
- We design a novel training strategy to adapt InterCLIP for a Memory-Enhanced Predictor (MEP). This strategy enables the integration of dynamic dual-channel memory, which stores valuable historical knowledge of test samples and leverages this memory for more precise and informed predictions.
- Our extensive experiments on the more reliable benchmark, MMSD2.0, demonstrate that InterCLIP-MEP outperforms existing state-of-the-art methods.

Related Work

Early work in sarcasm detection primarily focused on textual data (Bouazizi and Ohtsuki 2015; Poria et al. 2016; Amir et al. 2016; Wu et al. 2018; Tay et al. 2018; Baziotis et al. 2018). With the rise of social media, detecting sarcasm from text-image data has become increasingly challenging, leading to the development of several multi-modal approaches (Schifanella et al. 2016; Cai, Cai, and Wan 2019; Xu, Zeng, and Mao 2020; Pan et al. 2020; Liang et al. 2021, 2022; Liu, Wang, and Li 2022; Qin et al. 2023; Wen, Jia, and Yang 2023; Tian et al. 2023; Wei et al. 2024). Schifanella et al. (2016) were among the first to use multi-modal posts from social platforms to identify sarcasm clues from both text and images. Cai, Cai, and Wan (2019) introduced the MMSD benchmark for multi-modal sarcasm detection, demonstrating its effectiveness with a hierarchical fusion model incorporating image attributes. This benchmark has been widely used in subsequent studies (Xu, Zeng, and Mao 2020; Pan et al. 2020; Liang et al. 2021, 2022; Liu, Wang, and Li 2022; Qin et al. 2023; Wen, Jia, and Yang 2023; Tian et al. 2023; Wei et al. 2024). Further research expanded on MMSD, exploring dependencies and external knowledge, using advanced models, and introducing graph-based methods to enhance performance (Xu, Zeng, and Mao 2020; Pan et al. 2020; Liang et al. 2021, 2022; Liu, Wang, and Li 2022). However, MMSD has been proven to contain spurious cues that could bias models (Qin et al. 2023). To address

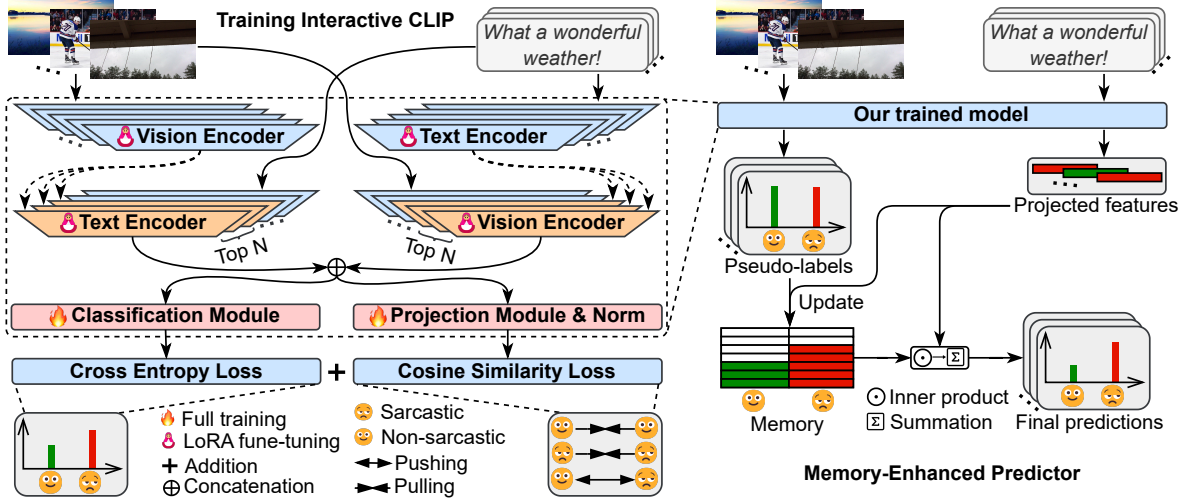


Figure 2: Overview of our framework. The left part of the figure shows the overall structure and training process of Interactive-CLIP. The right part illustrates the process of MEP identifying sarcastic samples.

this, Qin et al. (2023) introduced MMSD2.0 benchmark, which removed these cues and corrected mislabeled samples. They observed a significant performance drop when re-evaluating state-of-the-art methods on MMSD2.0 and proposed the need for more stable multi-modal sarcasm detection methods. Motivated by the work of Qin et al. (2023), we introduce the InterCLIP-MEP framework for more reliable multi-modal sarcasm detection.

Methodology

In this paper, we introduce InterCLIP-MEP, a novel framework for multi-modal sarcasm detection that combines interactive cross-modal encoding with memory-enhanced prediction. An overview of InterCLIP-MEP is illustrated in Figure 2. Our approach leverages a variant of CLIP, called Interactive CLIP (InterCLIP), which enhances the original CLIP architecture by embedding representations from one modality into the encoder of the other modality, resulting in more interactive representations. InterCLIP enables a nuanced understanding of the interaction between text and image. To facilitate memory-enhanced prediction, we design a novel training strategy, integrating a classification module and a projection module, with InterCLIP serving as the backbone. These modules are trained to identify sarcastic samples while constructing a latent space where features of the same class are clustered together and those of different classes are distinctly separated. For the prediction phase, InterCLIP-MEP employs a Memory-Enhanced Predictor (MEP) that leverages historical knowledge for final predictions. Instead of relying solely on the classification module to identify sarcasm, MEP compares the features of the current sample with those stored in memory, thereby enhancing the accuracy of sarcasm detection.

Interactive CLIP

We introduce Interactive CLIP (InterCLIP), which can condition text or image encoder to interact with representations

from the other modality, enhancing the capture of interactive information crucial for identifying sarcasm.

The input to InterCLIP is a text-image pair $\mathcal{P} = (T, I)$, where T represents a piece of text and I represents an image. Here, for simplicity, we do not consider the case of batch inputs. The text encoder \mathcal{T} extracts the vanilla text representation \mathbf{F}_t :

$$\mathbf{F}_t = \mathcal{T}(T) = \{h_{\text{bos}}^t(t_{\text{bos}}), h_1^t(t_1), \dots, h_n^t(t_n), h_{\text{eos}}^t(t_{\text{eos}})\}, \quad (1)$$

where t_i denotes a text token, n is the length of T after tokenization, t_{bos} and t_{eos} are special tokens required by the text encoder. Here, $h_i^t(\cdot) \in \mathbb{R}^{d_t}$ represents the d_t -dimensional encoded representation of the corresponding token t_i , with i ranging from 1 to n , including the beginning-of-sequence (bos) and end-of-sequence (eos) tokens. The vision encoder \mathcal{V} extracts the vanilla image representation \mathbf{F}_v :

$$\mathbf{F}_v = \mathcal{V}(I) = \{h_{\text{cls}}^v(p_{\text{cls}}), h_1^v(p_1), \dots, h_m^v(p_m)\}, \quad (2)$$

where I is processed into multiple patches p_i , m is the number of patches, and p_{cls} is a special token required by the visual encoder. Here, $h_i^v(\cdot) \in \mathbb{R}^{d_v}$ represents the d_v -dimensional encoded representation of the corresponding p_i , with i ranging from 1 to m , including the classification (cls) token. Specifically, both \mathbf{F}_t and \mathbf{F}_v are representations from the final layer outputs of their respective encoders. Conditioning on \mathbf{F}_t or \mathbf{F}_v , we can obtain the interactive text representation $\tilde{\mathbf{F}}_t$ or the interactive image representation $\tilde{\mathbf{F}}_v$:

$$\tilde{\mathbf{F}}_t = \mathcal{T}(T|\mathbf{F}_v), \tilde{\mathbf{F}}_v = \mathcal{V}(I|\mathbf{F}_t). \quad (3)$$

We use $\tilde{h}_i^t(\cdot) \in \mathbb{R}^{d_t}$ and $\tilde{h}_i^v(\cdot) \in \mathbb{R}^{d_v}$ to denote the re-encoded interactive representations of each text token and image patch, respectively.

Specifically, we condition only the top- n self-attention layers of the text or vision encoder, where n is a hyperparameter that will be analyzed in subsequent sections. The

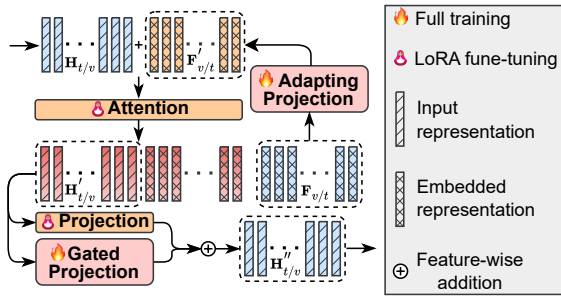


Figure 3: Structure of the conditional self-attention layer.

structure of the conditioned self-attention layers is illustrated in Figure 3. We denote the input representations to the self-attention layers as $\mathbf{H}_{t/v}$, which are the output representations from the previous layer. The previous layer can either be conditioned or non-conditioned. Due to the dimensional mismatch between the embedded representations $\mathbf{F}_{v/t}$ and the corresponding encoder representation space, we introduce an adapting projection layer $\mathcal{F}_{t/v}$ to project $\mathbf{F}_{v/t}$ into the appropriate representation space.

To fuse the input representations $\mathbf{H}_{t/v}$ with the projected embedded representations $\mathbf{F}'_{v/t} = \mathcal{F}_{t/v}(\mathbf{F}_{v/t})$, we concatenate them and feed them into the attention layer to obtain the transformed representations. We then extract the transformed input representations $\mathbf{H}'_{t/v}$ from the output. Following Ganz et al. (2024), we apply a gated projection layer $\mathcal{G}_{t/v}$ along with the self-attention’s projection head $\mathcal{H}_{t/v}$ using a learnable gating mechanism to compute the self-attention output representation $\mathbf{H}''_{t/v}$.

Given the similarity between the self-attention layers of the vision encoder and the text encoder, we use the text encoder \mathcal{T} to illustrate the process as follows:

$$\mathbf{F}'_v = \mathcal{F}_t(\mathbf{F}_v), \mathbf{F}_v \in \mathbb{R}^{m \times d_v}, \mathbf{F}'_v \in \mathbb{R}^{m \times d_t}, \quad (4)$$

$$\begin{aligned} \mathbf{H}'_t &= \text{Attn}_t(\mathbf{H}_t \oplus \mathbf{F}'_v)_{[n]}, \\ \mathbf{H}_t, \mathbf{H}'_t &\in \mathbb{R}^{n \times d_t}, \mathbf{H}_t \oplus \mathbf{F}'_v \in \mathbb{R}^{(n+m) \times d_t}, \end{aligned} \quad (5)$$

$$\mathbf{H}''_t = \mathcal{H}_t(\mathbf{H}'_t) + \mathcal{G}_t(\mathbf{H}'_t) \cdot \tanh(\beta_t), \mathbf{H}''_t \in \mathbb{R}^{n \times d_t}. \quad (6)$$

Here, \oplus denotes the concatenation operation, and β_t is a learnable parameter initialized to 0 to ensure training stability. The subsequent computation follows the original CLIP (Radford et al. 2021), ultimately yielding the interactive representations $\tilde{\mathbf{F}}_t$.

InterCLIP has three distinct modes to achieve the final fused feature $\tilde{h}^f \in \mathbb{R}^{d_t+d_v}$:

- **T2V:** The text encoder extracts the vanilla text representation \mathbf{F}_t . This text representation is then embedded into the vision encoder to obtain the conditioned vision representation $\tilde{\mathbf{F}}_v$. The final fused representation \tilde{h}^f is formed by concatenating $h_{\text{eos}}^t(t_{\text{eos}})$ and $\tilde{h}_{\text{cls}}^v(p_{\text{cls}})$.

- **V2T:** The vision encoder extracts the vanilla image representation \mathbf{F}_v . This image representation is then embedded into the text encoder to obtain the conditioned text representation $\tilde{\mathbf{F}}_t$. The final fused representation \tilde{h}^f is formed by concatenating $\tilde{h}_{\text{eos}}^t(t_{\text{eos}})$ and $h_{\text{cls}}^v(p_{\text{cls}})$.
- **Two-way (TW):** The text and vision encoders extract the vanilla text and image representations \mathbf{F}_t and \mathbf{F}_v , respectively. These representations are then embedded into the vision and text encoders to obtain the conditioned image representation $\tilde{\mathbf{F}}_v$ and text representation $\tilde{\mathbf{F}}_t$. The final fused representation \tilde{h}^f is formed by concatenating $\tilde{h}_{\text{eos}}^t(t_{\text{eos}})$ and $\tilde{h}_{\text{cls}}^v(p_{\text{cls}})$.

We will analyze the effectiveness of these three modes of interaction in the experimental analysis.

Training Strategy

As shown in Figure 2 (left), to adapt InterCLIP for memory-enhanced prediction, we introduce a novel training strategy. Using InterCLIP as the backbone to obtain fused features of the samples, we introduce a classification module and a projection module.

The classification module \mathcal{F}_c calculates the probability of a sample being sarcastic or non-sarcastic:

$$\hat{y} = \text{softmax}(\mathcal{F}_c(\tilde{H}^f)), \quad (7)$$

where $\tilde{H}^f \in \mathbb{R}^{N \times (d_t+d_v)}$ represents the fused representations of a batch of samples, and N denotes the batch size. We optimize \mathcal{F}_c using binary cross-entropy loss:

$$\mathcal{L}^c = -\frac{1}{N} \sum_{i=1}^N [y_i \log(\hat{y}_{i,1}) + (1 - y_i) \log(1 - \hat{y}_{i,1})], \quad (8)$$

where y_i denotes the label of the i -th sample, with sarcastic labeled as 1 and non-sarcastic as 0, and \hat{y}_i denotes the prediction for the i -th sample. The projection module \mathcal{F}_p maps \tilde{H}^f into a latent feature space:

$$\hat{H}^f = \text{norm}(\mathcal{F}_p(\tilde{H}^f)), \quad \hat{H}^f \in \mathbb{R}^{N \times d_f}, \quad (9)$$

where $\text{norm}(\cdot)$ denotes L2 normalization, and d_f represents the dimension of the projected features. In this space, cosine distance between features of the same class is minimized, while the distance between features of different classes is maximized. We use a label-aware cosine similarity loss to optimize \mathcal{F}_p :

$$\begin{aligned} \mathcal{L}^p &= \text{mean}(\hat{H}_P^f \cdot \hat{H}_N^{fT}) + \text{mean}(1 - \hat{H}_P^f \cdot \hat{H}_P^{fT}) \\ &\quad + \text{mean}(1 - \hat{H}_N^f \cdot \hat{H}_N^{fT}), \end{aligned} \quad (10)$$

where \hat{H}_P^f and \hat{H}_N^f represent the projected fused features of positive and negative samples, respectively.

We fully train the modules \mathcal{F}_c , \mathcal{F}_p , the adapting projection layer $\mathcal{F}_{t/v}$, the gated projection layer $\mathcal{G}_{t/v}$, and the parameters $\beta_{t/v}$. We use LoRA (Hu et al. 2022) to fine-tune parts of the weight matrices \mathbf{W} in the self-attention modules of all encoders, specifically various combinations of W_q , W_k , W_v , and W_o . We consider \mathbf{W} and the rank r of LoRA as hyperparameters for our study. All modules are optimized by minimizing the joint loss:

$$\mathcal{L} = \mathcal{L}^c + \mathcal{L}^p. \quad (11)$$

Algorithm 1: Memory-Enhanced Predictor

Input: Memory size L , Learned InterCLIP model, classification module \mathcal{F}_c and projection module \mathcal{F}_p

Output: Final prediction \hat{y}^p

```

1: Initialize memory  $\mathcal{M} \in \mathbf{0}^{2 \times L \times d_f}$ 
2: Initialize index  $\mathcal{I} \in \mathbf{0}^2$ 
3: Initialize entropy records  $\mathcal{C} \in \mathbf{0}^{2 \times L}$ 
4: for  $i \leftarrow 1$  to  $N_{\text{test}}$  do
5:    $\tilde{h}_i^f \leftarrow \text{InterCLIP}(\mathcal{P}_i)$ 
6:    $\hat{y}_i \leftarrow \text{softmax}(\mathcal{F}_c(\tilde{h}_i^f))$ 
7:    $\ell_{\text{pse}_i} \leftarrow \arg \max_j (\hat{y}_{i,j}), j \in \{0, 1\}$ 
8:    $c_i \leftarrow -\hat{y}_{i,0} \log \hat{y}_{i,0} - \hat{y}_{i,1} \log \hat{y}_{i,1}$ 
9:    $\hat{h}_i^f \leftarrow \text{norm}(\mathcal{F}_p(\tilde{h}_i^f))$ 
10:  if  $\mathcal{I}[\ell_{\text{pse}_i}] < L$  then
11:     $\mathcal{M}[\ell_{\text{pse}_i}][\mathcal{I}[\ell_{\text{pse}_i}]] \leftarrow \hat{h}_i^f$ 
12:     $\mathcal{C}[\ell_{\text{pse}_i}][\mathcal{I}[\ell_{\text{pse}_i}]] \leftarrow c_i$ 
13:     $\mathcal{I}[\ell_{\text{pse}_i}] \leftarrow \mathcal{I}[\ell_{\text{pse}_i}] + 1$ 
14:  else
15:     $j \leftarrow \text{GetMaxIdx}(\mathcal{C}[\ell_{\text{pse}_i}])$ 
16:    if  $c_i < \mathcal{C}[\ell_{\text{pse}_i}][j]$  then
17:       $\mathcal{M}[\ell_{\text{pse}_i}][j] \leftarrow \hat{h}_i^f$ 
18:       $\mathcal{C}[\ell_{\text{pse}_i}][j] \leftarrow c_i$ 
19:    end if
20:  end if
21:   $\text{logits} \leftarrow [\sum_{k=0}^{\mathcal{I}[0]} (\hat{h}_i^f \mathcal{M}[0]^T)_k, \sum_{k=0}^{\mathcal{I}[1]} (\hat{h}_i^f \mathcal{M}[1]^T)_k]$ 
22:   $\hat{y}_i^p \leftarrow \text{softmax}(\text{logits})$ 
23:  yield  $\hat{y}_i^p$ 
24: end for

```

Memory-Enhanced Predictor

As depicted in Figure 2 (right), we present a Memory-Enhanced Predictor (MEP) that builds upon the learned InterCLIP, along with the classification module and the projection module, leveraging the valuable historical knowledge of test samples to enhance sarcasm detection.

The detailed computational process of MEP is provided in Algorithm 1, where N_{test} denotes the number of test samples. MEP uses the trained InterCLIP to extract fused features of the samples. It utilizes the classification module \mathcal{F}_c to assign a pseudo-label ℓ_{pse_i} to each sample \mathcal{P}_i and the projection module \mathcal{F}_p to obtain the sample’s projected feature \hat{h}_i^f . To store valuable projected features of test samples as historical knowledge, MEP maintains a dynamic fixed-length dual-channel memory $\mathcal{M} \in \mathcal{R}^{2 \times L \times d_f}$, where L is the memory length per channel. The first channel stores projected features of non-sarcastic samples, while the second channel stores those of sarcastic samples. Based on the pseudo-label ℓ_{pse_i} , the appropriate memory channel $\mathcal{M}[\ell_{\text{pse}_i}]$ is selected for updating. If the selected channel has available space, the sample’s projected features are added directly, and the prediction entropy is recorded. If the memory is full, the prediction entropy of all samples in the memory is compared with that of the current sample, replacing the samples with the highest entropy as necessary. Finally, the current sample’s projected features are combined with the historical features

	All	Sarcastic	Non-sarcastic
Train	19812	9572	10240
Validation	2410	1042	1368
Test	2409	1037	1372

Table 1: Statistics of the dataset from the MMSD2.0 benchmark (Qin et al. 2023).

stored in both memory channels \mathcal{M} using cosine similarity to yield the final prediction.

Experiment

Experimental Settings

Datasets. We use the dataset from the MMSD2.0 benchmark (Qin et al. 2023), which is an improved version of the dataset originally introduced by Cai, Cai, and Wan (2019). We present the statistics of the dataset in Table 1.

Metrics. Following Liu, Wang, and Li (2022), we use accuracy (Acc.), precision (P), recall (R), and F1-score (F1) as metrics to evaluate the performance of our model.

Baselines. We compare the effectiveness of the InterCLIP-MEP framework against several uni-modal and multi-modal methods. For text modality methods, we compare with TextCNN (Kim 2014), Bi-LSTM (Graves and Schmidhuber 2005), SMSD (Xiong et al. 2019), and RoBERTa (Liu et al. 2019). For image modality methods, we compare with ResNet (He et al. 2015) and ViT (Dosovitskiy et al. 2020). For state-of-the-art multi-modal methods, we compare with the following:

- HFM (Cai, Cai, and Wan 2019): A hierarchical fusion model integrating text and image features.
- Att-BERT (Pan et al. 2020): A model using an attention mechanism to capture sarcasm incongruity.
- CMGCN (Liang et al. 2022): A method that constructs a cross-modal graph and employs a graph convolutional network.
- HKE (Liu, Wang, and Li 2022): A hierarchical framework utilizing multi-head cross-attention and graph neural networks.
- DIP (Wen, Jia, and Yang 2023): A dual incongruity perceiving network that extracts sarcastic information from factual and affective levels.
- DynRT (Tian et al. 2023): A dynamic routing transformer network for multi-modal sarcasm detection.
- Multi-view CLIP (Qin et al. 2023): A method adapted to CLIP for capturing multi-view sarcasm cues.
- G²SAM (Wei et al. 2024): A method using global graph-based semantic awareness and leveraging historical knowledge from training samples for multi-modal sarcasm detection.

Modality	Method	Acc. (%)	F1 (%)	P (%)	R (%)
Text	TextCNN* (Kim 2014)	71.61	69.52	64.62	75.22
	Bi-LSTM* (Graves and Schmidhuber 2005)	72.48	68.05	68.02	68.08
	SMSD* (Xiong et al. 2019)	73.56	69.97	68.45	71.55
	RoBERTa* (Liu et al. 2019)	79.66	76.21	76.74	75.70
Image	ResNet* (He et al. 2015)	65.50	57.58	61.17	54.39
	ViT* (Dosovitskiy et al. 2020)	72.02	69.72	65.26	74.83
Text-Image	HFM* (Cai, Cai, and Wan 2019)	70.57	66.88	64.84	69.05
	Att-BERT* (Pan et al. 2020)	80.03	77.04	76.28	77.82
	CMGCN* (Liang et al. 2022)	79.83	76.90	75.82	78.01
	HKE* (Liu, Wang, and Li 2022)	76.50	72.25	73.48	71.07
	DIP [†] (Wen, Jia, and Yang 2023)	80.59	78.23	75.52	81.14
	DynRT [†] (Tian et al. 2023)	70.37	68.55	63.02	75.15
	Multi-view CLIP* (Qin et al. 2023)	85.64	84.10	80.33	88.24
	G ² SAM [†] (Wei et al. 2024)	79.43	78.07	72.04	85.20
	InterCLIP-MEP w/o Inter ($L = 1024$)	86.05	84.81	79.83	90.45
	InterCLIP-MEP w/ TW ($L = 128$)	85.51	84.26	79.15	90.07
	InterCLIP-MEP w/ V2T ($L = 640$)	86.26	85.00	80.17	90.45
	InterCLIP-MEP w/ T2V ($L = 1024$)	86.72	85.61	80.20	91.80

Table 2: Main results. We use * to indicate that the results are taken from Qin et al. (2023). [†] indicates the results obtained by running this method on the MMSD2.0 benchmark (Qin et al. 2023).

Param.	Value
r	8
top- n	4
d_f	1024
\mathbf{W}	W_k, W_v, W_o
Epoch	3
Batch size	64
Learning rate	5e-4
LoRA learning rate	1e-4

Table 3: Hyperparameter settings.

Implementation Details

We implement model training and testing using PyTorch Lightning¹. We construct InterCLIP leveraging the Transformers library (Wolf et al. 2020), specifically utilizing the clip-vit-base-patch32² model from the HuggingFace Hub³. We optimize model parameters using AdamW (Loshchilov and Hutter 2017), setting the learning rate to 1e-4 for the LoRA fine-tuning modules and 5e-4 for other trainable modules. We employ a cosine annealing scheduler with warmup to dynamically adjust the learning rate, with warmup steps constituting the first 20% of the total optimization steps and the minimum learning rate set to 1% of the initial rate. For the modules $\mathcal{G}_{t/v}$, $\mathcal{F}_{t/v}$, \mathcal{F}_c , and \mathcal{F}_p , we use simple multi-layer perceptrons (MLPs). We perform

training with a batch size of 64 for 3 epochs. We run all experiments on a machine with an NVIDIA RTX 4090 GPU.

Main Results

The main results are shown in Table 2. To validate the effectiveness of our InterCLIP-MEP framework, we conduct experiments using the original CLIP as the backbone instead of InterCLIP, referred to as InterCLIP-MEP w/o Inter. We compare this configuration with three interaction modes of InterCLIP: InterCLIP-MEP w/ V2T, InterCLIP-MEP w/ T2V, and InterCLIP-MEP w/ TW.

For each experiment, we condition only the top four layers of the self-attention modules, with the projection dimension d_f set to 1024. We set the rank r of LoRA to 8, fine-tuning the self-attention module weight matrices \mathbf{W} , specifically W_k , W_v , and W_o . For the memory size L of the MEP, we select the optimal size from $\mathbf{L} = \{128, 256, 384, 512, 640, 768, 896, 1024, 1152, 1280\}$. Relevant hyperparameters are summarized in Table 3.

Our framework consistently outperforms or matches the performance of state-of-the-art methods, whether using InterCLIP or the original CLIP as the backbone, as shown in Table 2. This demonstrates the effectiveness of our training strategy and MEP. Methods InterCLIP-MEP w/ V2T and InterCLIP-MEP w/ T2V outperform InterCLIP-MEP w/o Inter, indicating that InterCLIP more effectively captures text-image interactions. Additionally, InterCLIP-MEP w/ T2V outperforms InterCLIP-MEP w/ V2T, likely due to the complexity of the visual space, which poses challenges for the projection layer in mapping visual representations into the text encoder space effectively. We observe that InterCLIP-MEP w/ TW performs worse than InterCLIP-

¹<https://lightning.ai/>

²<https://huggingface.co/openai/clip-vit-base-patch32>

³<https://huggingface.co/models>

Method	Acc. (%)	F1 (%)
<i>InterCLIP-MEP w/o Inter</i>		
BASLINE	86.05	84.81
w/o Proj	85.76	84.43
w/o MEP	85.39	83.99
w/o LoRA	82.44	77.73
<i>InterCLIP-MEP w/ TW</i>		
BASLINE	85.51	84.26
w/o Proj	85.43	84.05
w/o MEP	85.22	83.79
w/o LoRA	76.42	74.37
<i>InterCLIP-MEP w/ V2T</i>		
BASLINE	86.26	85.00
w/o Proj	85.68	84.22
w/o MEP	86.26	84.78
w/o LoRA	73.31	72.22
<i>InterCLIP-MEP w/ T2V</i>		
BASLINE	86.72	85.61
w/o Proj	86.22	84.51
w/o MEP	86.26	84.82
w/o LoRA	75.13	71.79

Table 4: Ablation study results of InterCLIP-MEP. BASELINE represents the results of the corresponding method without any ablation.

MEP w/o Inter, possibly because embedding representations within both encoders increases learning difficulty compared to unidirectional methods. In summary, InterCLIP with T2V interaction, combined with our training strategy and MEP yields the most promising results.

Ablation Study

To further validate the effectiveness of InterCLIP-MEP, we remove the projection module \mathcal{F}_p and train only the classification module \mathcal{F}_c for prediction, denoted as w/o Proj. To test the necessity of using LoRA (Hu et al. 2022) for fine-tuning, we keep the rest of InterCLIP-MEP unchanged and freeze all self-attention weight matrices of InterCLIP, denoted as w/o LoRA, always selecting the optimal memory size L for the MEP during inference. To evaluate the effectiveness of the MEP, we train both \mathcal{F}_p and \mathcal{F}_c but use only \mathcal{F}_c during inference, denoted as w/o MEP.

Table 4 reports all results. All variants show performance declines compared to the baseline, demonstrating the importance of each module in the InterCLIP-MEP framework. For methods InterCLIP-MEP w/ TW and InterCLIP-MEP w/o Inter, the w/o MEP variant performed worse than the w/o Proj variant. However, for methods InterCLIP-MEP w/ T2V and InterCLIP-MEP w/ V2T, the w/o MEP variant performs better than the w/o Proj variant. This suggests that backbones with strong image-text interaction capabilities benefit from training the classification module \mathcal{F}_c along with the projection module \mathcal{F}_p , even without using MEP

W	Mean Acc. (%)	Mean F1 (%)
W_q	85.14	83.99
W_k	85.09	84.00
W_v	85.34	84.24
W_o	85.39	84.23
W_q, W_k	85.36	84.16
W_q, W_v	85.63	84.40
W_q, W_o	85.73	84.49
W_k, W_o	85.67	84.43
W_v, W_o	85.73	84.54
W_k, W_v	85.70	84.51
W_q, W_k, W_o	85.92	84.63
W_q, W_v, W_o	85.87	84.60
W_q, W_k, W_v	86.05	84.75
W_k, W_v, W_o	86.14	84.92
W_q, W_k, W_v, W_o	85.82	84.55

Table 5: Average results of fine-tuning different weight matrices **W** across four baseline methods.

Method	Mean Acc. (%)	Mean F1 (%)
w/o Inter	85.49	84.32
w/ TW	85.66	84.44
w/ V2T	85.62	84.41
w/ T2V	85.78	84.55

Table 6: Average results of four baseline methods for fine-tuning different weight matrices **W**.

during inference. We also find that not using LoRA to fine-tune the self-attention modules results in significant performance loss, indicating that the original CLIP’s vanilla space is not directly suitable for the sarcasm detection task.

Hyperparameter Study

In this section, we investigate the impact of different hyperparameter settings on model performance. Keeping the other hyperparameters constant as shown in Table 3, we fine-tune all possible weight matrices **W** for methods using original CLIP and different interaction modes of Interactive-CLIP as the backbone. We consistently select the optimal memory size from **L** for MEP. We calculate the average metrics for different methods and different weight matrices. The results are presented in Table 5 and Table 6. We observe that fine-tuning the weight matrices W_k, W_v, W_o and using the T2V interaction mode of Interactive-CLIP are the best choices for our InterCLIP-MEP framework.

We further investigate the method using Interactive-CLIP with T2V interaction as the backbone. Keeping the other hyperparameters constant, we condition different top-n layers of the self-attention modules. We also study the impact of different projection dimensions d_f , different LoRA ranks r , and different memory sizes L on the InterCLIP-MEP w/ T2V method. We present all results in Figure 4. Figure 4(a) shows that conditioning the top four self-attention layers yields the best results. From Figure 4(b), a rank of 8 is

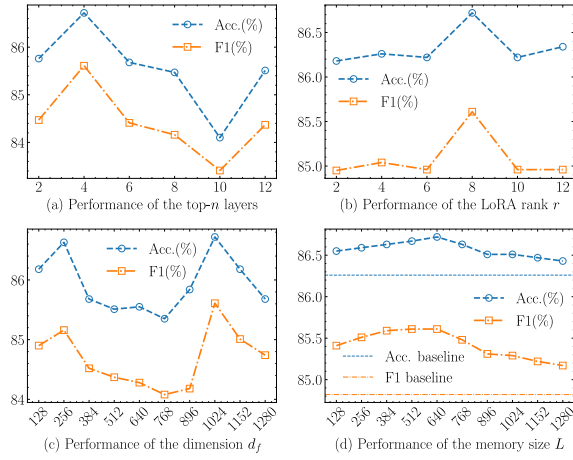


Figure 4: Hyperparameter study curves for InterCLIP-MEP w/ T2V. Figure 4(d) compares results with those from using only the classification module \mathcal{F}_c for prediction.



Sample	Prediction
 <p>i'm pretty sure this cookie cake isn't big enough.</p>	GT: 😊 MEP: 😊 ✓ \mathcal{F}_c : 😊 (entropy=0.58) ✗
<p>Teacher: You can't write an essay overnight.</p> <p>Exam: You have one hour to write an essay.</p> <p>everything is a test</p>	GT: 😊 MEP: 😊 ✓ \mathcal{F}_c : 😊 (entropy=0.60) ✗
 <p>the trees are so beautiful i shed a tear</p>	GT: 😊 MEP: 😊 ✓ \mathcal{F}_c : 😊 (entropy=0.66) ✗

Figure 5: Case study of InterCLIP-MEP.

optimal. Figure 4(c) indicates the projection dimension is best at 256 or 1024. Figure 4(d) reveals that a memory size of 640 in MEP outperforms others, confirming the value of historical sample knowledge.

Case Study

As shown in Figure 5, we select three examples to further demonstrate the robustness of InterCLIP-MEP. We observe that direct predictions through the classification module \mathcal{F}_c result in high entropy and incorrect outcomes. However, because the InterCLIP-MEP framework leverages the Memory-Enhanced Predictor (MEP) to utilize historical knowledge of test samples during inference, This approach effectively mitigates the issue for cases where the classification module fails to correctly identify the results by using the historical knowledge of the test samples.

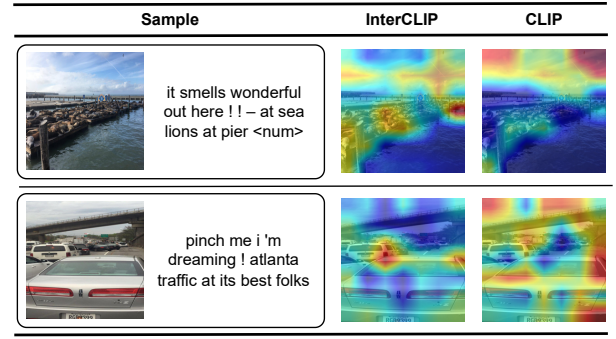


Figure 6: Visual comparison between Interactive-CLIP and original CLIP.

Visualization

To further validate that Interactive-CLIP can more effectively capture the interactive information between text and images compared to original CLIP, thereby aiding in the detection of sarcasm cues, we visualize the areas of focus during the inference process of the visual model in Figure 6. We observe that in the first example, which complains about the unpleasant odor caused by the sea lions, Interactive-CLIP focuses more accurately on the location of the sea lions compared to the original CLIP. In the second example, which complains about traffic congestion, Interactive-CLIP correctly focuses on the distribution of cars on the road, whereas the original CLIP's focus is scattered.

Conclusion and Future Work

In this paper, we propose a novel framework for robust multi-modal sarcasm detection, termed InterCLIP-MEP. We introduce Interactive CLIP (InterCLIP) as the backbone for extracting sample representations. Unlike the original CLIP, InterCLIP embeds representations from different modalities into the encoder, effectively capturing the intricate interactions between text and image. For inference, we introduce a Memory-Enhanced Predictor (MEP) that leverages historical knowledge of test samples to enhance inference, providing a more robust alternative to directly using the classification module for sarcasm recognition. This approach significantly improves the detection of sarcastic samples. Our experimental results demonstrate that InterCLIP-MEP achieves state-of-the-art performance on the MMSD2.0 benchmark. In future work, we plan to extend our approach to sarcasm recognition tasks across additional modalities, such as speech and video.

Acknowledgments

The research described in the paper received funding from the Anhui Provincial Natural Science Foundation through Grant No. 2308085MF220. Additionally, it was co-supported by the Anhui University Natural Science Foundation, which provided funding through Grant Nos. 2022AH050972 and KJ2021A0516.

References

- Amir, S.; Wallace, B. C.; Lyu, H.; and Silva, P. C. M. J. 2016. Modelling context with user embeddings for sarcasm detection in social media. *arXiv preprint arXiv:1607.00976*.
- Baziotis, C.; Athanasiou, N.; Papalampidi, P.; Kolovou, A.; Paraskevopoulos, G.; Ellinas, N.; and Potamianos, A. 2018. Ntua-slp at semeval-2018 task 3: Tracking ironic tweets using ensembles of word and character level attentive rnns. *arXiv preprint arXiv:1804.06659*.
- Bouazizi, M.; and Ohtsuki, T. 2015. Sarcasm detection in twitter:” all your products are incredibly amazing!!!”-are they really? In *2015 IEEE global communications conference (GLOBECOM)*, 1–6. IEEE.
- Cai, Y.; Cai, H.; and Wan, X. 2019. Multi-Modal Sarcasm Detection in Twitter with Hierarchical Fusion Model. In *Annual Meeting of the Association for Computational Linguistics*.
- Devlin, J.; Chang, M.-W.; Lee, K.; and Toutanova, K. 2019. BERT: Pre-training of Deep Bidirectional Transformers for Language Understanding. *North American Chapter of the Association for Computational Linguistics*.
- Dosovitskiy, A.; Beyer, L.; Kolesnikov, A.; Weissenborn, D.; Zhai, X.; Unterthiner, T.; Dehghani, M.; Minderer, M.; Heigold, G.; Gelly, S.; Uszkoreit, J.; and Housby, N. 2020. An Image is Worth 16x16 Words: Transformers for Image Recognition at Scale. *arXiv preprint arXiv: 2010.11929*.
- Ganz, R.; Kittenplon, Y.; Aberdam, A.; Avraham, E. B.; Nuriel, O.; Mazor, S.; and Litman, R. 2024. Question Aware Vision Transformer for Multimodal Reasoning. *arXiv preprint arXiv:2402.05472*.
- Gibbs, R. W.; and Colston, H. L. 2007. Irony in Language and Thought : A Cognitive Science Reader.
- Gibbs, R. W.; and O’Brien, J. E. 1991. Psychological aspects of irony understanding. *Journal of Pragmatics*, 16: 523–530.
- Graves, A.; and Schmidhuber, J. 2005. Framewise phoneme classification with bidirectional LSTM and other neural network architectures. *Neural Networks*, 18(5): 602–610. IJCNN 2005.
- He, K.; Zhang, X.; Ren, S.; and Sun, J. 2015. Deep Residual Learning for Image Recognition. *arXiv preprint arXiv: 1512.03385*.
- Hu, E. J.; Shen, Y.; Wallis, P.; Allen-Zhu, Z.; Li, Y.; Wang, S.; Wang, L.; and Chen, W. 2022. LoRA: Low-Rank Adaptation of Large Language Models. In *The Tenth International Conference on Learning Representations, ICLR 2022, Virtual Event, April 25-29, 2022*. OpenReview.net.
- Kim, Y. 2014. Convolutional Neural Networks for Sentence Classification. In Moschitti, A.; Pang, B.; and Daelemans, W., eds., *Proceedings of the 2014 Conference on Empirical Methods in Natural Language Processing (EMNLP)*, 1746–1751. Doha, Qatar: Association for Computational Linguistics.
- Liang, B.; Lou, C.; Li, X.; Gui, L.; Yang, M.; and Xu, R. 2021. Multi-modal sarcasm detection with interactive in-modal and cross-modal graphs. In *Proceedings of the 29th ACM international conference on multimedia*, 4707–4715.
- Liang, B.; Lou, C.; Li, X.; Yang, M.; Gui, L.; He, Y.; Pei, W.; and Xu, R. 2022. Multi-Modal Sarcasm Detection via Cross-Modal Graph Convolutional Network. In *Annual Meeting of the Association for Computational Linguistics*.
- Liu, H.; Wang, W.; and Li, H. 2022. Towards Multi-Modal Sarcasm Detection via Hierarchical Congruity Modeling with Knowledge Enhancement. In *Conference on Empirical Methods in Natural Language Processing*.
- Liu, Y.; Ott, M.; Goyal, N.; Du, J.; Joshi, M.; Chen, D.; Levy, O.; Lewis, M.; Zettlemoyer, L.; and Stoyanov, V. 2019. RoBERTa: A Robustly Optimized BERT Pretraining Approach. *arXiv preprint arXiv: 1907.11692*.
- Loshchilov, I.; and Hutter, F. 2017. Decoupled Weight Decay Regularization. *arXiv preprint arXiv: 1711.05101*.
- Muecke, D. C. 1982. *Irony and the Ironic*. New York: Methuen.
- Pan, H.; Lin, Z.; Fu, P.; Qi, Y.; and Wang, W. 2020. Modeling Intra and Inter-modality Incongruity for Multi-Modal Sarcasm Detection. In Cohn, T.; He, Y.; and Liu, Y., eds., *Findings of the Association for Computational Linguistics: EMNLP 2020*, 1383–1392. Online: Association for Computational Linguistics.
- Pang, B.; Lee, L.; et al. 2008. Opinion mining and sentiment analysis. *Foundations and Trends® in information retrieval*, 2(1–2): 1–135.
- Poria, S.; Cambria, E.; Hazarika, D.; and Vij, P. 2016. A deeper look into sarcastic tweets using deep convolutional neural networks. *arXiv preprint arXiv:1610.08815*.
- Qiao, Y.; Jing, L.; Song, X.; Chen, X.; Zhu, L.; and Nie, L. 2023. Mutual-Enhanced Incongruity Learning Network for Multi-Modal Sarcasm Detection. In *AAAI Conference on Artificial Intelligence*.
- Qin, L.; Huang, S.; Chen, Q.; Cai, C.; Zhang, Y.; Liang, B.; Che, W.; and Xu, R. 2023. MMSD2.0: Towards a Reliable Multi-modal Sarcasm Detection System. In Rogers, A.; Boyd-Graber, J.; and Okazaki, N., eds., *Findings of the Association for Computational Linguistics: ACL 2023*, 10834–10845. Toronto, Canada: Association for Computational Linguistics.
- Radford, A.; Kim, J. W.; Hallacy, C.; Ramesh, A.; Goh, G.; Agarwal, S.; Sastry, G.; Askell, A.; Mishkin, P.; Clark, J.; et al. 2021. Learning transferable visual models from natural language supervision. In *International conference on machine learning*, 8748–8763. PMLR.
- Schifanella, R.; De Juan, P.; Tetreault, J.; and Cao, L. 2016. Detecting sarcasm in multimodal social platforms. In *Proceedings of the 24th ACM international conference on Multimedia*, 1136–1145.
- Tay, Y.; Tuan, L. A.; Hui, S. C.; and Su, J. 2018. Reasoning with sarcasm by reading in-between. *arXiv preprint arXiv:1805.02856*.
- Tian, Y.; Xu, N.; Zhang, R.; and Mao, W. 2023. Dynamic Routing Transformer Network for Multimodal Sarcasm Detection. In *Annual Meeting of the Association for Computational Linguistics*.

Tsur, O.; Davidov, D.; and Rappoport, A. 2010. ICWSM—a great catchy name: Semi-supervised recognition of sarcastic sentences in online product reviews. In *Proceedings of the International AAAI Conference on Web and Social Media*, volume 4, 162–169.

Wei, Y.; Yuan, S.; Zhou, H.; Wang, L.; Yan, Z.; Yang, R.; and Chen, M. 2024. G2SAM: Graph-Based Global Semantic Awareness Method for Multimodal Sarcasm Detection. *Proceedings of the AAAI Conference on Artificial Intelligence*, 38(8): 9151–9159.

Wen, C.; Jia, G.; and Yang, J. 2023. Dip: Dual incongruity perceiving network for sarcasm detection. In *Proceedings of the IEEE/CVF Conference on Computer Vision and Pattern Recognition*, 2540–2550.

Wolf, T.; Debut, L.; Sanh, V.; Chaumond, J.; Delangue, C.; Moi, A.; Cistac, P.; Rault, T.; Louf, R.; Funtowicz, M.; Davison, J.; Shleifer, S.; von Platen, P.; Ma, C.; Jernite, Y.; Plu, J.; Xu, C.; Scao, T. L.; Gugger, S.; Drame, M.; Lhoest, Q.; and Rush, A. M. 2020. Transformers: State-of-the-Art Natural Language Processing. In *Proceedings of the 2020 Conference on Empirical Methods in Natural Language Processing: System Demonstrations*, 38–45. Online: Association for Computational Linguistics.

Wu, C.; Wu, F.; Wu, S.; Liu, J.; Yuan, Z.; and Huang, Y. 2018. Thu_ngn at semeval-2018 task 3: Tweet irony detection with densely connected lstm and multi-task learning. In *Proceedings of The 12th International Workshop on Semantic Evaluation*, 51–56.

Xiong, T.; Zhang, P.; Zhu, H.; and Yang, Y. 2019. Sarcasm Detection with Self-matching Networks and Low-rank Bilinear Pooling. In *The World Wide Web Conference, WWW '19*, 2115–2124. New York, NY, USA: Association for Computing Machinery. ISBN 9781450366748.

Xu, N.; Zeng, Z.; and Mao, W. 2020. Reasoning with multimodal sarcastic tweets via modeling cross-modality contrast and semantic association. In *Proceedings of the 58th annual meeting of the association for computational linguistics*, 3777–3786.